Published in final edited form as:

Glia. 2024 January ; 72(1): 156–166. doi:10.1002/glia.24467.

YAP and TAZ regulate remyelination in the central nervous system.

Jiayue Hong[1,*], **Jules M Kirkland**[1,*], **Jenica Acheta**[1,*], **Leandro N Marziali**[2], **Brianna Beck**[1], **Haley Jeanette**[1], **Urja Bhatia**[1], **Grace Davis**[1], **Jacob Herron**[1], **Clémence Roué**[1], **Charly Abi-Ghanem**[1], **M Laura Feltri**[2,3], **Kristen Zuloaga**[1], **Marie E Bechler**[4], **Yannick Poitelon**[1,#], **Sophie Belin**[1,#]

[1]Albany Medical College, Department of Neuroscience and Experimental Therapeutics, Albany, NY, 12208, USA.

[2]Institute for Myelin and Glia Exploration, Dept. Biochemistry, University at Buffalo, Buffalo, NY, 14203, USA.

[3]Neurology, Jacobs School of Medicine and Biomedical Sciences, University at Buffalo, Buffalo, NY, 14203, USA.

[4]Department of Cell and Developmental Biology, and Department of Neuroscience and Physiology State University of New York Upstate Medical University, Syracuse, NY, 13210, USA.

Abstract

Myelinating cells are sensitive to mechanical stimuli from their extracellular matrix. Ablation of YAP and TAZ mechanotransducers in Schwann cells abolishes the axon–Schwann cell recognition, myelination, and remyelination in the peripheral nervous system. It was unknown if YAP and TAZ are also required for myelination and remyelination in the central nervous system. Here we define the importance of oligodendrocyte YAP and TAZ *in vivo*, by specific deletion in oligodendroglial cells in adult oligodendrocytes during myelin repair. Blocking YAP and TAZ expression in oligodendrocyte lineage cells did not affect animal viability or any major defects on oligodendrocyte maturation and myelination. However, using a mouse model of demyelination/remyelination, we demonstrate that YAP and TAZ modulate the capacity of oligodendrocytes to remyelinate axons, particularly during the early stage of the repair process, when oligodendrocyte proliferation is most important. These results indicate that YAP and TAZ signaling is necessary for effective remyelination of the mouse brain.

Corresponding authors: Sophie Belin and Yannick Poitelon, Albany Medical College, Department of Neuroscience and Experimental Therapeutics, 47 New Scotland Avenue, MC-136, Albany, NY, 12208, belins@amc.edu, poitely@amc.edu, 518-262-3555.

*, #These authors contributed equally to this work.

Author contributions

Sophie Belin and Yannick Poitelon designed research, analyzed data, and wrote the manuscript; Haley Jeanette, Leandro Marziali, Jules Kirkland, and Sophie Belin performed experiments with Jenica Acheta, Jiayue Hong, Brianna Beck, Urja Bhatia, Grace Davis, Jacob Herron, Clemence Roué and Charly Abi Ghanem assistance; Kristen Zuloaga contributed to technical tools for the data analysis; Maria Laura Feltri contributed to generation of mutant mice at the beginning of the project; Leandro Marziali and Marie Bechler critically reviewed the manuscript.

Conflict of Interest

The authors declare no competing financial interests.

Graphical Abstract

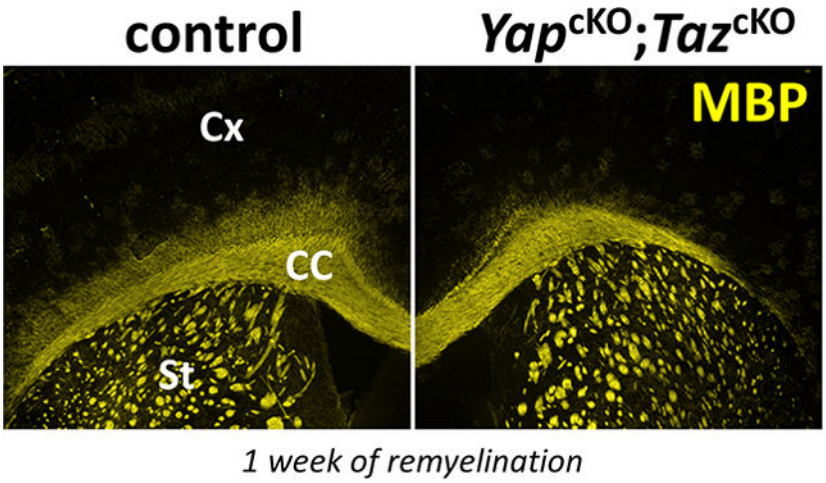

Keywords

Yap; Taz; myelin; oligodendrocyte; remyelination

Introduction

Oligodendrocytes (OLs) and Schwann cells are the glial cell in the central nervous system (CNS) and peripheral nervous system (PNS), with similar roles in producing myelin to insulate axons and facilitate fast propagation of action potentials. OL and Schwann cell proliferation, migration, differentiation, maturation, and myelination are tightly regulated by intrinsic signals, such as transcription factors and epigenetic modulators, as well as extrinsic signals such as growth factors, hormones, and mechanical cues (reviewed in Tsai & Casaccia, 2019).

Mechanical cues can activate YAP and TAZ, transcription coactivators of the Hippo pathway. When YAP and TAZ are phosphorylated, they are inactive. Upon activation, YAP and TAZ are dephosphorylated and shuttle from the cytosol to the nuclei and interact with transcription factors of the TEAD family (reviewed in Feltri, Weaver, Belin, & Poitelon, 2021). In the PNS, YAP and TAZ are both essential for axon-Schwann cell recognition, proliferation and myelination (Deng et al., 2017; Fernando et al., 2016; Grove et al., 2017; Poitelon et al., 2016). More specifically, YAP and TAZ promote myelination by regulating transcription of myelin proteins and lipid synthesis regulators, synergistically with SOX10 and EGR2 (Deng et al., 2017; Fernando et al., 2016; Grove et al., 2017; Lopez-Anido et al., 2016; Poitelon et al., 2016; Wu et al., 2018). In addition, YAP and TAZ also play a role in peripheral nerve regeneration and remyelination following nerve crush injury (Grove, Lee, Zhao, & Son, 2020; Jeanette et al., 2021; Mindos et al., 2017).

In the CNS, many studies have shown that YAP and TAZ regulate the self-renewal and maintenance of neural stem cells (Bao, He, Wang, Huang, & Yuan, 2017; Cao, Pfaff, & Gage, 2008; Ding, Weynans, Bossing, Barros, & Berger, 2016; Gil-Ranedo et al., 2019; Han

et al., 2015; Lavado et al., 2013; Lavado et al., 2018; Van Hateren et al., 2011; Yao et al., 2014). In addition, YAP was shown to be expressed by OLs *in vitro* (Jagielska et al., 2017; Ong et al., 2020; Shimizu et al., 2016; Urbanski et al., 2016). Shimizu et al. showed that overexpression of YAP in OLs decreased the number of mature OLs *in vivo.* The authors also demonstrated that knock-down of YAP in OLs limits the extension of primary processes *in vitro,* suggesting that it impairs their capacity to myelinate (Shimizu et al., 2016). Ong et al. showed *in vitro* that YAP is a mediator of mechanical cues from the environment in myelinating OLs, but not in differentiating OL precursor cells (OPCs) (Ong et al., 2020). Finally, animals ablated for both *Yap* and *Taz* in adult myelinating Schwann cells and OLs (*Yap*$^{f/f}$; *Taz*$^{f/f}$; *Plp1*-Cre^{ER}) exhibit severe weight loss, tremors, ataxia and mortality within two weeks (Deng et al., 2017; Grove et al., 2017; Grove et al., 2020; Jeanette et al., 2021). However, preliminary exploration by Deng et al. did not detect overt myelin abnormalities in the adult corpus callosum or spinal cord of these animals. Thus, while YAP and TAZ respond to mechanical stress and impact oligodendrocytes differentiation *in vitro*, there is a need to clarify if YAP and TAZ modulate *in vivo* OL lineage cell proliferation, maturation, myelination, and remyelination.

In this study, we used two different genetic mouse models to selectively inactivate YAP and TAZ (*Yap*$^{f/f}$; *Taz*$^{f/f}$; *Olig2*-Cre and *Yap*$^{f/f}$; *Taz*$^{f/f}$; *Plp1*-Cre^{ER}) to clarify the function of YAP and TAZ in developing (*Olig2*-Cre) and myelinating OLs (*Plp1*-Cre^{ER}). We also studied the role of YAP and TAZ in myelination and remyelination following cuprizone treatment. Supported by morphological, cellular, and molecular data, we show here that ablation of YAP and TAZ has no major effect on myelination. However, we found that ablation of YAP and TAZ in OL lineage cells significantly affects OPC proliferation and delays the remyelination process, suggesting that YAP and TAZ are required in the OPCs of the adult brain to properly remyelinate the CNS.

Materials and Methods

Animal Models.

This study was carried out in accordance with the principles of the Basel Declaration and recommendations of ARRIVE guidelines issued by the NC3Rs and approved by the Albany Medical College Institutional Animal Care and Use Committee (no. 20–08001). *Yap*$^{f/f}$ and *Taz*$^{f/f}$ mice (Reginensi et al., 2013) were derived to a congenic C57BL/6J background (as described in Poitelon et al., 2016), bred with *Plp1*-Cre^{ER} (Jackson Laboratory, #005975) (Doerflinger, Macklin, & Popko, 2003) or *Olig2*-Cre mice (Jackson Laboratory, #025567) (Zawadzka et al., 2010) to generate *Yap*$^{f/f}$; *Taz*$^{f/f}$; *Plp1*-Cre^{ER} (Jeanette et al., 2021) and *Yap*$^{f/f}$; *Taz*$^{f/f}$; *Olig2*-Cre. Genotyping of mutant mice was performed by PCR on tail genomic DNA (Poitelon et al., 2016). Tamoxifen (Sigma-Aldrich, T5648) was injected into *Yap*$^{f/f}$; *Taz*$^{f/f}$; *Plp1*-Cre^{ER} mice. A 20 mg/ml solution of tamoxifen was prepared in autoclaved corn oil. This solution was injected intraperitoneally at a concentration of 100 mg/kg body weight starting on post-natal day 40 (P40). A total of 5 injections were performed, spaced apart every 12 hours. The resulting mutant mice were compared with their littermates injected with corn oil only, and to *Yap*$^{f/f}$; *Taz*$^{f/f}$ animals injected with tamoxifen. Animals were housed in cages of 5 with 12/12 hours light/dark cycles. No

animals were excluded from the study. Equal numbers of males and females were included in the study. Mutant and control littermates from both sexes were culled at the indicated ages, and optic nerves and brains were collected.

Cuprizone treatment in mice.

Postnatal day 40 (P40) mice were fed with powder chow, freshly prepared with 0.2 % copper chelator agent Cuprizone (Sigma-Aldrich, C9012) for 6 weeks. Half of each experimental group was randomly selected and culled after 6 weeks of the cuprizone demyelination period to analyze YAP and TAZ function during demyelination. The other half were back to normal diet and allowed to recover for up to 4 weeks with normal pellet chow to analyze YAP and TAZ function during remyelination. Body weight of mice was closely monitored prior and during the 6 weeks of cuprizone treatment.

Electron microscopy.

Mutant and control littermates were euthanized at the indicated ages, and optic nerves were dissected. Optic nerves were fixed in 2% buffered glutaraldehyde and post fixed in 1% osmium tetroxide. After alcohol dehydration, the samples were embedded in EPON resin. Ultrathin sections (80nm – 85 nm thick) were stained with saturated uranyl acetate and lead citrate and examined by electron microscopy for morphometry analysis. For all morphological assessments, at least 3 animals per genotype were analyzed. For g-ratio analysis of optic nerves (axon diameter/fiber diameter), ultrathin section images were acquired with a FEI Tecnai F20 transmission electron microscope. Axon and fiber diameters were quantified from TEM images using the ImageJ software (imagej.nih.gov/ij). G-ratios were determined for at least 100 fibers chosen randomly per animal.

Primary cultures of mouse cortical oligodendrocytes.

Oligodendrocyte precursors cells (OPC) were isolated from P3–5 mouse brain cortices by immunopanning according to Emery and Dugas, 2013 with slight modifications (Emery & Dugas, 2013). P3–5 mouse brains were obtained, meninges removed, and cortices dissected. Next, the cortices were dissociated into a single cell suspension using Miltenyi's Neural Tissue Dissociation Kit (P) (Miltenyi, 130–092-628). Microglia were removed from the cell suspension by panning with BSL-1 (5 μg/mL) (Vector Laboratories, L-1100) coated plates and OPCs were purified with anti-PDGFRα 1/4000 (BD Pharmingen, 558774) coated plates. Next, OPCs were plated onto poly-D-lysine coated (PDL) - 20 μg/mL (Sigma-Aldrich, P0899) coverslips and incubated at 37 °C, 5 % CO_2 in SATO based media containing: DMEM (Thermo Fisher Scientific, 11965092), 0.1 mg/mL bovine serum albumin (Sigma-Aldrich, A4161), 0.1 mg/mL Transferrin (Sigma-Aldrich, T1147), 16 μg/mL Putrescine (Sigma-Aldrich, P5780), 60 ng/mL Progesterone (Sigma, P8783), 40 ng/mL Sodium Selenite (Sigma, S5261), 10 ng/mL d-Biotin (Sigma-Aldrich, B4639), 5 μg/mL insulin, 1 mM sodium pyruvate (Thermo Fisher Scientific, 11360–070), 5 μg/mL N-Acetyl-L-cysteine (Sigma-Aldrich, A8199), 1X Trace elements B (Cellgo, 99–175-CI), 4.2 ng/mL forskolin (Sigma-Aldrich, F6886) and 1X B27 (Thermo Fisher Scientific, 17504044). OPCs were kept under proliferation conditions for 48 hours by adding 10 ng/mL CNTF (PeproTech, 450–13), 1 ng/mL NT3 (PeproTech, 450–03) and 20 ng/mL PDGF-AA (PeproTech, 100–13A) to the basal media. Next, OPCs were allowed to differentiate for

48 hours by adding 10 ng/mL CNTF, 15 nM T3 (Sigma-Aldrich, T6397) and 10 μg/mL L-ascorbic acid (Sigma-Aldrich, A4544) to the basal media.

Immunohistochemistry.

All animals were anesthetized with 2.5 % trimoboethanol (avertin), injected intraperitoneally, and then perfused with iced cold 0.9% saline followed by 4% of paraformaldehyde (PFA) via the left ventricle. Brains and spinal cords (vertebrae L3) were post fixed overnight in 4 % of PFA at 4 °C, followed by immersion in 30% sucrose for 72 hours. The optic nerves were incubated in 5% sucrose for 15 minutes and 20% sucrose overnight, as in (Belin, Herron, et al., 2019; Poitelon et al., 2018). Brains, spinal cords and optic nerves were equilibrated in OCT compound and frozen in nitrogen vapors before storage at −80 ºC. Coronal brain slices, spinal cord cross sections of 50 μm thick and optic nerve cross sections of 10 μm thick were prepared using a cryostat (Leica Biosystems, CM1950). For myelin staining in the brain and spinal cord, free-floating sections were incubated in a blocking solution (5 % fetal bovine serum and 0.2 % Triton X-100 in PBS) for 2 hours at room temperature and incubated with primary antibodies in an incubation solution (2 % fetal bovine serum and 0.2 % Triton X-100 in PBS) for 2 hours at room temperature. For nuclear staining in the brain and spinal cord, free floating sections were incubated in a blocking solution (10% Donkey serum and 0.2% Triton X-100 in PBS) for 2 hours at room temperature. When using mouse primary antibody, 1:40 mouse-on-mouse (MOM) blocking agent (Vector lab, BMK-2202) was added to the blocking solution. For myelin and nuclear staining in the optic nerves, dry mounted sections were incubated in a blocking solution (20% fetal bovine serum, 1% Bovine Serum Albumin, 0.1% triton X-100) and permeabilized with cold methanol for 30 seconds. For OL lineage cells, cells were fixed in 4 % PFA, 0.5 % dodecyltrimethylammonium chloride, blocked for 1 hour in 5 % normal goat serum, 0.1 % Triton X-100. The following primary antibodies were used in this study: anti-TAZ 1/1000 (ProteinTech, 23306–1-AP), anti-YAP 1/100 (Cell Signaling, 4912), anti-MBP 1/1000 (Biolegend, 808401), anti-PLP-1 1/500 (Abcam, PA3–151), anti-MOG 1/500 (Millipore, MAB5680), anti-OLIG2 1/500 (Abcam, AB9610 and R&D, AF2418), anti-SOX10 1/1000 (Cell Signaling, 89356), anti-KI67 1/1000 (Abcam, ab15580), and anti-CC1 1/1000 (Abcam, Ab16794). Sections were then rinsed in PBS and incubated with Alexa 488, 555 and 633-conjugated secondary antibodies for 1 or 2 hours at room temperature. The sections were then rinsed with PBS followed by a counterstain with DAPI. The sections were mounted on microscopy slides using coverslips and mounting medium (Invitrogen, 00–4958-02). Images from cultures OLs were acquired using a Leica confocal microscope, model SP5II. Images for quantifications from brains, spinal cords and optic nerves were acquired using the Axio observer fluorescent microscope (Carl Zeiss Microscopy, Jena Germany) The staining intensity for myelin proteins and the number of positive cells were determined at a depth of 1.1 mm to bregma into the central area of the corpus callosum (0.6 mm^2), in the motor cortex area (0.6 mm^2) and in the striatum (0.6 mm^2). The integrated fluorescence intensity was calculated as the product of the area and mean pixel intensity using ImageJ (http://imagej.nih.gov/ij). All quantification of positive cells and fluorescent intensity results were determined from at least four brains per experimental group.

Western Blotting.

Optic nerves and corpus callosum were collected and frozen in liquid nitrogen, pulverized and resuspended in lysis buffer [lysis buffer 95 mM NaCl, 25 mM Tris-HCl pH 7.4 10 mM EDTA, 2% SDS, 1% Protease Inhibitor Cocktail (Roche Diagnostic)] (Acheta, Hong, et al., 2022; Belin, Ornaghi, et al., 2019). Protein lysates were centrifuged at 15,000 g for 30 min at 4 °C. Supernatant protein concentrations were determined by bicinchoninic acid assay protein assay according to the manufacturer's instructions. Equal amounts of homogenates were diluted 3:1 in 4 X Laemmli (250 mM Tris-HCl pH 6.8, 8 % sodium dodecyl sulfate, 8 % β-Mercaptoethanol, 40 % Glycerol, 0.02 % Bromophenol Blue), denatured 5 min at 100 °C, resolved on SDS-polyacrylamide gel and electro-blotted onto PVDF membrane. Blots were then blocked with 5 % bovine serum albumin in 1X PBS, 0.05 % Tween-20 and incubated overnight with the following appropriate antibodies: anti-TAZ 1/1000 (ProteinTech, 23306–1-AP), anti-YAP 1/200 (Santa Cruz, sc-101199), anti-MBP 1/1000 (Millipore, AB5864), anti-PLP1 1/500 (Abcam, ab28486), anti-MOG 1/500 (Millipore, MAB5680), anti-Calnexin 1/3000 (Sigma, C4731), anti-GAPDH 1/2000 (Sigma, G9545). Membranes were then rinsed in 1X PBS and incubated for 1 h with secondary antibodies. Blots were developed using ECL or ECL plus (GE Healthcare). Western blots were quantified using Image J software (http://imagej.nih.gov/ij). Full blots are presented in Supplementary Fig. 1.

Statistical Analysis.

Experiments were not randomized, but data collection and analysis were performed blind to the conditions of the experiments. Data were analyzed using GraphPad Prism 6.01. Data are presented as mean ± standard error of the mean (S.E.M.). No statistical methods were used to predetermine sample sizes, but our sample sizes are similar to those generally employed in the field. Two-tailed Student's t-test was used for statistical analysis of the differences between two groups. Values of P-value ≤ 0.05 were considered to represent a significant difference.

Results

YAP and TAZ are expressed in the CNS and OLs.

To clarify the role of YAP and TAZ in OLs, we first looked at YAP and TAZ expression level in the CNS. We investigated both the corpus callosum and optic nerve, two regions of the CNS rich in OLs and myelin. In developing optic nerve, we found that YAP and TAZ were expressed at low level between postnatal day 6 (P6) and P10, when OLs start myelinating; then YAP and TAZ expression increased from P15 up to P90. In comparison, in developing corpus callosum, YAP and TAZ are stably expressed from P6 to P90. These data indicate that YAP and TAZ are expressed in CNS regions rich in OLs (Fig. 1A, Supplementary Fig. 1). In agreement with those observations, we detected YAP and TAZ expression *in vitro* in both OPCs and mature OLs, with YAP and TAZ localization being nuclear as well as cytoplasmic (Fig. 1B, Supplementary Fig. 2).

To further investigate the role of YAP and TAZ in OLs in the adult CNS, we used the double knockout mouse model *Yap*$^{f/f}$; *Taz*$^{f/f}$; *Plp1*-Cre^{ER}. *Plp1*-Cre^{ER} expression is conditional

following intraperitoneal injections of tamoxifen and allows for temporally controlled ablation of YAP and TAZ in adult myelinated glial cells (both OL lineage and Schwann cells). This mouse model is only viable for about 14 days following tamoxifen injection, which limits the window of analysis for the study of YAP and TAZ function in the CNS (Deng et al., 2017; Grove et al., 2017; Grove et al., 2020; Jeanette et al., 2021). *Yap*$^{f/f}$; *Taz*$^{f/f}$; *Plp1*-Cre^{ER} animals received 5 injections of tamoxifen, one every 12 hours at postnatal day 40. We analyzed YAP and TAZ protein levels in optic nerve 13 days after tamoxifen injection. Only YAP protein levels were visibly reduced in *Yap*$^{f/f}$; *Taz*$^{f/f}$; *Plp1*-Cre^{ER} (Fig. 1C, Supplementary Fig. 1), suggesting that TAZ is also expressed by other CNS cells, such as astrocytes and endothelial cells (Zhang et al., 2014). Collectively these data support that both YAP and TAZ are expressed in OLs in the adult CNS. However, as only YAP protein levels are significantly affected in the *Yap*$^{f/f}$; *Taz*$^{f/f}$; *Plp1*-Cre^{ER} mouse model, the data suggest a high proportion of non-OL cells express TAZ protein in the brain.

YAP and TAZ are not essential for OL maturation and myelination in the CNS.

Because the *Yap*$^{f/f}$; *Taz*$^{f/f}$; *Plp1*-Cre^{ER} mouse model is only viable for about 14 days following tamoxifen injection (Deng et al., 2017; Grove et al., 2017; Grove et al., 2020; Jeanette et al., 2021), the window of analysis for the study of YAP and TAZ function in the CNS was limited to 13 days post recombination. Thus, the role of YAP and TAZ in OLs was evaluated by immunohistochemistry, in animals at 53 days of age (P40 plus 13 days after tamoxifen injection). Compared with control littermates, the fluorescent signal for MBP was not reduced in the corpus callosum, cortex, striatum, optic nerves and spinal cord of *Yap*$^{f/f}$; *Taz*$^{f/f}$; *Plp1*-Cre^{ER} animals (Fig. 2, Supplementary Fig. 3). Also, the length and thickness of the corpus callosum were not significantly different in *Yap*$^{f/f}$; *Taz*$^{f/f}$; *Plp1*-Cre^{ER} animals and their controls (Fig. 2C). The myelination of the *Yap*$^{f/f}$; *Taz*$^{f/f}$; *Plp1*-Cre^{ER} CNS was also evaluated by immunohistochemistry for myelin oligodendrocyte glycoprotein (MOG) and proteolipid protein1 (PLP1). No significant differences were observed for these proteins in the brain (Supplementary Fig. 4). To analyze the effect of YAP and TAZ deletion on OLs, the total number of OL lineage cells (OLIG2-positive cells) was analyzed in the brain, spinal cord, and optic nerve. The total number of OLIG2-positive cells was unaffected by the absence of YAP and TAZ in OLs in all CNS areas (Fig. 2A, Supplementary Fig. 3). The myelination of the *Yap*$^{f/f}$; *Taz*$^{f/f}$; *Plp1*-Cre^{ER} animals was also assessed by electron microscopy. The degree of myelination was analyzed by calculating the g-ratio of myelinated axons in optic nerve (Fig. 3). The *Yap*$^{f/f}$; *Taz*$^{f/f}$; *Plp1*-Cre^{ER} animals did not show any changes in the mean g-ratio of myelinated axons (Fig. 3B) or in the average diameter of myelinated axons (Fig. 3C).

To further investigate the role of YAP and TAZ at an earlier time point in brain development, we used the double knockout mouse model *Yap*$^{f/f}$; *Taz*$^{f/f}$; *Olig2*-Cre, which allows site-specific recombination in all oligodendrocyte lineage cells and motor neurons, as early as embryonic day 10.5 (Dessaud et al., 2007; Zawadzka et al., 2010). Importantly, compared to *Yap*$^{f/f}$; *Taz*$^{f/f}$; *Plp1*-Cre^{ER} animals, the *Yap*$^{f/f}$; *Taz*$^{f/f}$; *Olig2*-Cre animals didn't display any weight loss, tremors, ataxia and mortality. Myelination was evaluated by immunohistochemistry at 7, 20, 40 and 60 days of age. Compared with control littermates, no significant differences were observed in the brain of *Yap*$^{f/f}$; *Taz*$^{f/f}$; *Olig2*-Cre for the

fluorescent signal for MBP, and in the number of OLIG2-positive cells or the dimensions of the corpus callosum at 20 days of age (Fig. 4) as well as at 7, 40 and 60 days of age (Supplementary Fig. 5). In addition, no differences were observed for the fluorescent signal for MBP and the number of OLIG2-positive cells in optic nerve (Supplementary Fig. 6). Overall, the results obtained with *Yap*$^{f/f}$; *Taz*$^{f/f}$; *Plp1*-Cre^{ER} and Yap$^{f/f}$; Taz$^{f/f}$; *Olig2*-Cre animals suggest that YAP and TAZ are not essential for OL maturation and myelin maintenance in the CNS.

YAP and TAZ are required for the remyelination of the adult mouse brain.

To determine how the loss of YAP and TAZ affects the remyelination potential of OLs in the adult mouse brain, we used the cuprizone model of demyelination and remyelination. We used P60 control (*Yap*$^{f/f}$; *Taz*$^{f/f}$) and *Yap*$^{f/f}$; *Taz*$^{f/f}$; *Olig2*-Cre mice, which did not present obvious myelination defects (Supplementary Fig. 5). Mice were treated with cuprizone for 6 weeks to induce demyelination. Brains were then collected for analysis after 6 weeks of cuprizone treatment and at 4 weeks of recovery in normal diet. 6 weeks of cuprizone treatment induced a severe demyelination in the brain of both control and *Yap*$^{f/f}$; *Taz*$^{f/f}$; *Olig2*-Cre mice, as well as weight loss (Fig. 5, Supplementary Fig. 7). A significant recovery in MBP, PLP and MOG levels was observed in the corpus callosum and cortex of both control and *Yap*$^{f/f}$; *Taz*$^{f/f}$; *Olig2*-Cre after the 4 weeks of remyelination following withdrawal of cuprizone treatment (Fig. 5). Yet *Yap*$^{f/f}$; *Taz*$^{f/f}$; *Olig2*-Cre mice showed significantly less MBP, PLP and MOG production than control mice in the cortex and in the lateral corpus callosum suggesting a delay in remyelination (Fig. 5,). These reductions were also observed by Western blot of myelin proteins (Fig. 5). We detected a decrease in the number of OLIG2-positive cells and OLIG2-positive cell proliferation during recovery in the corpus callosum and cortex of *Yap*$^{f/f}$; *Taz*$^{f/f}$; *Olig2*-Cre mice (Fig. 6), but not in the number of mature oligodendrocytes (CC1-positive and OLIG2-positive cells) (Fig. 6). Interestingly, absence of YAP and TAZ in oligodendrocytes appears to have a more severe effect in the corpus callosum than in the cortex (Fig. 6). We did not observe any increase in apoptosis in oligodendrocyte lineage in *Yap*$^{f/f}$; *Taz*$^{f/f}$; *Olig2*-Cre after the 2 weeks of remyelination following withdrawal of cuprizone treatment (data not shown). Collectively these data support that expression of both YAP and TAZ are required for the remyelination in the CNS, and for proliferation of oligodendrocyte precursors during remyelination.

Discussion

Although remyelination occurs, this process cannot be sustained and eventually fails in central nervous system myelin disorders such as progressive multiple sclerosis. Thus, understanding how the OLs integrate cues necessary for proper remyelination is critical to develop new means to treat patients with myelin disorders. Our knowledge regarding the integration of mechanical stimuli during remyelination has primarily come from *in vitro* models. In contrast, the conditional knockout mice described in this work allowed us to specifically study the *in vivo* consequences of YAP and TAZ deficit in the OL lineage during myelination and remyelination.

YAP and TAZ in myelinating glial cells.

The biological role of YAP and TAZ is cell, tissue, and biological context specific. They can have broad effects, as seen for Schwann cell proliferation, differentiation, myelination and remyelination (Deng et al., 2017; Fernando et al., 2016; Grove et al., 2017; Grove et al., 2020; Jeanette et al., 2021; Poitelon et al., 2016). Schwann cells share numerous similarities with OLs. However, there are important differences between OLs and Schwann cells in their embryological origin (*i.e.*: neural stem cells for OLs vs. neural crest cells for Schwann cells), development, mechanisms of wrapping, molecular composition, response to injury, and the distinct signaling pathways and transcription factors that regulate their differentiation and myelin formation (*e.g.*: OLIG1/2 and MYRF in OLs vs. POU3F1 and EGR2 in Schwann cells) (reviewed in Herbert & Monk, 2017). In accordance with these differences, diseases of myelin are in general restricted to myelinated fibers in the CNS or in the PNS (*e.g.*: Multiple Sclerosis, leukodystrophies in the CNS vs. Charcot-Marie-Tooth disease, Guillain-Barré Syndrome in the PNS). Most importantly some promyelinating pathways in the PNS have an opposite role on myelin formation in the CNS (*e.g.*: MLC2, KIF13B, DNM2) (Gerber et al., 2019; Noseda et al., 2013; Wang, Tewari, Einheber, Salzer, & Melendez-Vasquez, 2008). Therefore, despite YAP and TAZ being critically needed for Schwann cell biology, there was an outstanding gap to assess the function of YAP and TAZ in OLs and to determine if, like in the PNS, YAP and TAZ are also required for CNS myelination and remyelination. Our data show that, despite being expressed in the OL lineage, YAP and TAZ seem to be dispensable for myelin maintenance in the CNS. While we cannot exclude that ablation of YAP and TAZ in the developing brain of young animals could have an effect of OL proliferation, survival and differentiation, their ablation had no major effect of OL maturation and myelination. Yet, distinctively during repair, our data also show that ablation of YAP and TAZ significantly delays the remyelination process, suggesting that YAP and TAZ are required in the OL lineage of the adult brain to properly proliferate and myelinate the CNS after demyelination. It will be important for future studies to investigate these mechanisms in depth. First the defect in proliferation seen in oligodendrocyte lacking YAP and TAZ could come from a defect in the proliferation of oligodendrocyte lineage, or from a defect in the proliferation or migration of neural stem cells (Heng et al., 2020). Second, we observed the absence of YAP and TAZ in oligodendrocytes seems to affect more severely the oligodendrocyte proliferation in the corpus callosum compared to the cortex, thus suggesting a region-specific function for YAP and TAZ, with a more important role in controlling oligodendrocyte proliferation in whiter matter than in grey matter. Finally, while YAP and TAZ regulate myelin formation in the PNS through TEAD1 and EGR2 (Lopez-Anido et al., 2016), it is still unknown which transcriptional factors are partnering with YAP and TAZ to regulate remyelination.

YAP and TAZ regulation in OLs.

OLs like other cells in the CNS, are subjected to both tension forces (mediated by the cytoskeleton) and compression forces (mediated by the extracellular matrix and neighboring cells) during development and aging, and in pathological conditions (reviewed in Makhija, Espinosa-Hoyos, Jagielska, & Van Vliet, 2020). Numerous works have demonstrated that mechanical cues regulate myelinating glial cell migration, differentiation, proliferation, and myelination (Acheta, Bhatia, et al., 2022; Fernando et al., 2016; Hernandez et al., 2016;

Jagielska et al., 2017; Jagielska et al., 2012; Kim et al., 2020; Lourenco et al., 2016; Ong et al., 2020; Poitelon et al., 2016; Poitelon, Nunes, & Feltri, 2017; Rosenberg, Kelland, Tokar, De la Torre, & Chan, 2008; Urbanski, Brendel, & Melendez-Vasquez, 2019; Urbanski et al., 2016). In addition, changes in extracellular matrix deposition and composition may highly contribute to changes in mechanical properties and brain remyelination capacity, as demonstrated by prior work showing that acute demyelinated lesions following a 6-week cuprizone treatment are softer than healthy brain tissue (Urbanski et al., 2019).

Several studies have shown the involvement of constitutive signaling pathways such as YAP and TAZ to transduce mechanical signals into transcriptional regulation in OLs (Jagielska et al., 2017; Ong et al., 2020; Shimizu et al., 2016; Urbanski et al., 2016). In addition, proper amount of YAP and TAZ activation is paramount to regulate OL biology during development as both *in vitro* YAP knockdown and *in vivo* YAP overexpression can decrease the formation of OL processes (Shimizu et al., 2016).

Here, our work indicates that two mechanotransducers YAP and TAZ are also required for OL lineage proliferation and the remyelination of the CNS following cuprizone-induced demyelination, but not for oligodendrocyte maturation or differentiation. These results are somewhat surprising given that (i) a stiffer environment promotes the translocation of YAP to the nucleus in response to both tensile strain (Shimizu et al., 2016) and rigid substrates (Ong et al., 2020; Urbanski et al., 2016); (ii) acutely demyelinated brain is softer than healthy brain tissue (Urbanski et al., 2019). Yet, while mechanical cues may contribute to the regulation of YAP and TAZ, YAP and TAZ are regulated by non-mechanical signals from the HIPPO signaling pathways (Dobrokhotov, Samsonov, Sokabe, & Hirata, 2018; Feltri et al., 2021). In addition, it is possible that the functions of these other mechanosensitive pathways in OLs could predominate over YAP and TAZ in regulating the OL lineage (Hernandez et al., 2016; Segel et al., 2019; Velasco-Estevez et al., 2020).

In sum, there are more efforts needed to understand the mechanobiology of OLs. First it is essential to better characterize the contributors to the changes in mechanical environment, to OL mechanosensation, and mechanotransduction in diseases. Second, further studies should focus on characterizing these contributors *in vivo* or if done *in vitro* using materials at a stiffness within the pathophysiological range. Finally, it will be important to understand how OLs integrate mechanical cues together with biochemical signals.

Supplementary Material

Refer to Web version on PubMed Central for supplementary material.

Acknowledgements

This work was funded by NIH NINDS R01 NS110627 to Yannick Poitelon, and by National Multiple Sclerosis Society PP-1803-30535 pilot grant to Yannick Poitelon.

References

Acheta J, Bhatia U, Haley J, Hong J, Rich K, Close R, . . . Poitelon Y. (2022). Piezo channels contribute to the regulation of myelination in Schwann cells. Glia. doi:10.1002/glia.24251

Acheta J, Hong J, Jeanette H, Brar S, Yalamanchili A, Feltri ML, . . . Poitelon Y. (2022). Cc2d1b Contributes to the Regulation of Developmental Myelination in the Central Nervous System. Front Mol Neurosci, 15, 881571. doi:10.3389/fnmol.2022.881571 [PubMed: 35592111]

Bao XM, He Q, Wang Y, Huang ZH, & Yuan ZQ (2017). The roles and mechanisms of the Hippo/YAP signaling pathway in the nervous system. Yi Chuan, 39(7), 630–641. doi:10.16288/j.yczz.17-069 [PubMed: 28757477]

Belin S, Herron J, VerPlank JJS, Park Y, Feltri LM, & Poitelon Y. (2019). Corrigendum: YAP and TAZ Regulate Cc2d1b and Purbeta in Schwann Cells. Front Mol Neurosci, 12, 256. doi:10.3389/fnmol.2019.00256 [PubMed: 31680860]

Belin S, Ornaghi F, Shackleford G, Wang J, Scapin C, Lopez-Anido C, . . . Wrabetz L. (2019). Neuregulin 1 type III improves peripheral nerve myelination in a mouse model of congenital hypomyelinating neuropathy. Hum Mol Genet, 28(8), 1260–1273. doi:10.1093/hmg/ddy420 [PubMed: 30535360]

Cao X, Pfaff SL, & Gage FH (2008). YAP regulates neural progenitor cell number via the TEA domain transcription factor. Genes Dev, 22(23), 3320–3334. doi:10.1101/gad.1726608 [PubMed: 19015275]

Deng Y, Wu LMN, Bai S, Zhao C, Wang H, Wang J, . . . Lu QR (2017). A reciprocal regulatory loop between TAZ/YAP and G-protein Galphas regulates Schwann cell proliferation and myelination. Nat Commun, 8, 15161. doi:10.1038/ncomms15161 [PubMed: 28443644]

Dessaud E, Yang LL, Hill K, Cox B, Ulloa F, Ribeiro A, . . . Briscoe J. (2007). Interpretation of the sonic hedgehog morphogen gradient by a temporal adaptation mechanism. Nature, 450(7170), 717–720. doi:10.1038/nature06347 [PubMed: 18046410]

Ding R, Weynans K, Bossing T, Barros CS, & Berger C. (2016). The Hippo signalling pathway maintains quiescence in Drosophila neural stem cells. Nat Commun, 7, 10510. doi:10.1038/ncomms10510 [PubMed: 26821647]

Dobrokhotov O, Samsonov M, Sokabe M, & Hirata H. (2018). Mechanoregulation and pathology of YAP/TAZ via Hippo and non-Hippo mechanisms. Clin Transl Med, 7(1), 23. doi:10.1186/s40169-018-0202-9 [PubMed: 30101371]

Doerflinger NH, Macklin WB, & Popko B. (2003). Inducible site-specific recombination in myelinating cells. Genesis, 35(1), 63–72. doi:10.1002/gene.10154 [PubMed: 12481300]

Emery B, & Dugas JC (2013). Purification of oligodendrocyte lineage cells from mouse cortices by immunopanning. Cold Spring Harb Protoc, 2013(9), 854–868. doi:10.1101/pdb.prot073973 [PubMed: 24003195]

Feltri ML, Weaver MR, Belin S, & Poitelon Y. (2021). The Hippo pathway: Horizons for innovative treatments of peripheral nerve diseases. J Peripher Nerv Syst, 26(1), 4–16. doi:10.1111/jns.12431 [PubMed: 33449435]

Fernando RN, Cotter L, Perrin-Tricaud C, Berthelot J, Bartolami S, Pereira JA, . . . Tricaud N. (2016). Optimal myelin elongation relies on YAP activation by axonal growth and inhibition by Crb3/Hippo pathway. Nat Commun, 7, 12186. doi:10.1038/ncomms12186 [PubMed: 27435623]

Gerber D, Ghidinelli M, Tinelli E, Somandin C, Gerber J, Pereira JA, . . . Suter U. (2019). Schwann cells, but not Oligodendrocytes, Depend Strictly on Dynamin 2 Function. Elife, 8. doi:10.7554/eLife.42404

Gil-Ranedo J, Gonzaga E, Jaworek KJ, Berger C, Bossing T, & Barros CS (2019). STRIPAK Members Orchestrate Hippo and Insulin Receptor Signaling to Promote Neural Stem Cell Reactivation. Cell Rep, 27(10), 2921–2933 e2925. doi:10.1016/j.celrep.2019.05.023 [PubMed: 31167138]

Grove M, Kim H, Santerre M, Krupka AJ, Han SB, Zhai J, . . . Son YJ (2017). YAP/TAZ initiate and maintain Schwann cell myelination. Elife, 6. doi:10.7554/eLife.20982

Grove M, Lee H, Zhao H, & Son YJ (2020). Axon-dependent expression of YAP/TAZ mediates Schwann cell remyelination but not proliferation after nerve injury. Elife, 9. doi:10.7554/eLife.50138

Han D, Byun SH, Park S, Kim J, Kim I, Ha S, . . . Yoon K. (2015). YAP/TAZ enhance mammalian embryonic neural stem cell characteristics in a Tead-dependent manner. Biochem Biophys Res Commun, 458(1), 110–116. doi:10.1016/j.bbrc.2015.01.077 [PubMed: 25634692]

Heng BC, Zhang X, Aubel D, Bai Y, Li X, Wei Y, . . . Deng X. (2020). Role of YAP/TAZ in Cell Lineage Fate Determination and Related Signaling Pathways. Front Cell Dev Biol, 8, 735. doi:10.3389/fcell.2020.00735 [PubMed: 32850847]

Herbert AL, & Monk KR (2017). Advances in myelinating glial cell development. Curr Opin Neurobiol, 42, 53–60. doi:10.1016/j.conb.2016.11.003 [PubMed: 27930937]

Hernandez M, Patzig J, Mayoral SR, Costa KD, Chan JR, & Casaccia P. (2016). Mechanostimulation Promotes Nuclear and Epigenetic Changes in Oligodendrocytes. J Neurosci, 36(3), 806–813. doi:10.1523/JNEUROSCI.2873-15.2016 [PubMed: 26791211]

Jagielska A, Lowe AL, Makhija E, Wroblewska L, Guck J, Franklin RJM, . . . Van Vliet KJ (2017). Mechanical Strain Promotes Oligodendrocyte Differentiation by Global Changes of Gene Expression. Front Cell Neurosci, 11, 93. doi:10.3389/fncel.2017.00093 [PubMed: 28473753]

Jagielska A, Norman AL, Whyte G, Vliet KJ, Guck J, & Franklin RJ (2012). Mechanical environment modulates biological properties of oligodendrocyte progenitor cells. Stem Cells Dev, 21(16), 2905–2914. doi:10.1089/scd.2012.0189 [PubMed: 22646081]

Jeanette H, Marziali LN, Bhatia U, Hellman A, Herron J, Kopec AM, . . . Belin S. (2021). YAP and TAZ regulate Schwann cell proliferation and differentiation during peripheral nerve regeneration. Glia, 69(4), 1061–1074. doi:10.1002/glia.23949 [PubMed: 33336855]

Kim J, Adams AA, Gokina P, Zambrano B, Jayakumaran J, Dobrowolski R, . . . Kim HA (2020). Mechanical stretch induces myelin protein loss in oligodendrocytes by activating Erk1/2 in a calcium-dependent manner. Glia, 68(10), 2070–2085. doi:10.1002/glia.23827 [PubMed: 32170885]

Lavado A, He Y, Pare J, Neale G, Olson EN, Giovannini M, & Cao X. (2013). Tumor suppressor Nf2 limits expansion of the neural progenitor pool by inhibiting Yap/Taz transcriptional coactivators. Development, 140(16), 3323–3334. doi:10.1242/dev.096537 [PubMed: 23863479]

Lavado A, Park JY, Pare J, Finkelstein D, Pan H, Xu B, . . . Cao X. (2018). The Hippo Pathway Prevents YAP/TAZ-Driven Hypertranscription and Controls Neural Progenitor Number. Dev Cell, 47(5), 576–591 e578. doi:10.1016/j.devcel.2018.09.021 [PubMed: 30523785]

Lopez-Anido C, Poitelon Y, Gopinath C, Moran JJ, Ma KH, Law WD, . . . Svaren J. (2016). Tead1 regulates the expression of Peripheral Myelin Protein 22 during Schwann cell development. Hum Mol Genet, 25(14), 3055–3069. doi:10.1093/hmg/ddw158 [PubMed: 27288457]

Lourenco T, Paes de Faria J, Bippes CA, Maia J, Lopes-da-Silva JA, Relvas JB, & Graos M. (2016). Modulation of oligodendrocyte differentiation and maturation by combined biochemical and mechanical cues. Sci Rep, 6, 21563. doi:10.1038/srep21563 [PubMed: 26879561]

Makhija EP, Espinosa-Hoyos D, Jagielska A, & Van Vliet KJ (2020). Mechanical regulation of oligodendrocyte biology. Neurosci Lett, 717, 134673. doi:10.1016/j.neulet.2019.134673 [PubMed: 31838017]

Mindos T, Dun XP, North K, Doddrell RD, Schulz A, Edwards P, . . . Parkinson DB (2017). Merlin controls the repair capacity of Schwann cells after injury by regulating Hippo/YAP activity. J Cell Biol, 216(2), 495–510. doi:10.1083/jcb.201606052 [PubMed: 28137778]

Noseda R, Belin S, Piguet F, Vaccari I, Scarlino S, Brambilla P, . . . Bolino A. (2013). DDIT4/REDD1/RTP801 is a novel negative regulator of Schwann cell myelination. J Neurosci, 33(38), 15295–15305. doi:10.1523/JNEUROSCI.2408-13.2013 [PubMed: 24048858]

Ong W, Marinval N, Lin J, Nai MH, Chong YS, Pinese C, . . . Chew SY (2020). Biomimicking Fiber Platform with Tunable Stiffness to Study Mechanotransduction Reveals Stiffness Enhances Oligodendrocyte Differentiation but Impedes Myelination through YAP-Dependent Regulation. Small, 16(37), e2003656. doi:10.1002/smll.202003656

Poitelon Y, Lopez-Anido C, Catignas K, Berti C, Palmisano M, Williamson C, . . . Feltri ML (2016). YAP and TAZ control peripheral myelination and the expression of laminin receptors in Schwann cells. Nat Neurosci, 19(7), 879–887. doi:10.1038/nn.4316 [PubMed: 27273766]

Poitelon Y, Matafora V, Silvestri N, Zambroni D, McGarry C, Serghany N, . . . Feltri ML (2018). A dual role for Integrin alpha6beta4 in modulating hereditary neuropathy with liability to pressure palsies. J Neurochem, 145(3), 245–257. doi:10.1111/jnc.14295 [PubMed: 29315582]

Poitelon Y, Nunes GD, & Feltri ML (2017). Myelinating cells can feel disturbances in the force. Oncotarget, 8(4), 5680–5681. doi:10.18632/oncotarget.14240 [PubMed: 28031544]

Reginensi A, Scott RP, Gregorieff A, Bagherie-Lachidan M, Chung C, Lim DS, . . . McNeill H. (2013). Yap- and Cdc42-dependent nephrogenesis and morphogenesis during mouse kidney development. PLoS Genet, 9(3), e1003380. doi:10.1371/journal.pgen.1003380

Rosenberg SS, Kelland EE, Tokar E, De la Torre AR, & Chan JR (2008). The geometric and spatial constraints of the microenvironment induce oligodendrocyte differentiation. Proc Natl Acad Sci U S A, 105(38), 14662–14667. doi:10.1073/pnas.0805640105 [PubMed: 18787118]

Segel M, Neumann B, Hill MFE, Weber IP, Viscomi C, Zhao C, . . . Chalut KJ (2019). Niche stiffness underlies the ageing of central nervous system progenitor cells. Nature. doi:10.1038/s41586-019-1484-9

Shimizu T, Osanai Y, Tanaka KF, Abe M, Natsume R, Sakimura K, & Ikenaka K. (2016). YAP functions as a mechanotransducer in oligodendrocyte morphogenesis and maturation. Glia, 65(2), 360–374. doi:10.1002/glia.23096 [PubMed: 27807898]

Tsai E, & Casaccia P. (2019). Mechano-modulation of nuclear events regulating oligodendrocyte progenitor gene expression. Glia, 67(7), 1229–1239. doi:10.1002/glia.23595 [PubMed: 30734358]

Urbanski MM, Brendel MB, & Melendez-Vasquez CV (2019). Acute and chronic demyelinated CNS lesions exhibit opposite elastic properties. Sci Rep, 9(1), 999. doi:10.1038/s41598-018-37745-7 [PubMed: 30700777]

Urbanski MM, Kingsbury L, Moussouros D, Kassim I, Mehjabeen S, Paknejad N, & Melendez-Vasquez CV (2016). Myelinating glia differentiation is regulated by extracellular matrix elasticity. Sci Rep, 6, 33751. doi:10.1038/srep33751 [PubMed: 27646171]

Van Hateren NJ, Das RM, Hautbergue GM, Borycki AG, Placzek M, & Wilson SA (2011). FatJ acts via the Hippo mediator Yap1 to restrict the size of neural progenitor cell pools. Development, 138(10), 1893–1902. doi:10.1242/dev.064204 [PubMed: 21521736]

Velasco-Estevez M, Gadalla KKE, Linan-Barba N, Cobb S, Dev KK, & Sheridan GK (2020). Inhibition of Piezo1 attenuates demyelination in the central nervous system. Glia, 68(2), 356–375. doi:10.1002/glia.23722 [PubMed: 31596529]

Wang H, Tewari A, Einheber S, Salzer JL, & Melendez-Vasquez CV (2008). Myosin II has distinct functions in PNS and CNS myelin sheath formation. J Cell Biol, 182(6), 1171–1184. doi:10.1083/jcb.200802091 [PubMed: 18794332]

Wu LMN, Deng Y, Wang J, Zhao C, Wang J, Rao R, . . . Lu QR (2018). Programming of Schwann Cells by Lats1/2-TAZ/YAP Signaling Drives Malignant Peripheral Nerve Sheath Tumorigenesis. Cancer Cell, 33, this issue.

Yao M, Wang Y, Zhang P, Chen H, Xu Z, Jiao J, & Yuan Z. (2014). BMP2-SMAD signaling represses the proliferation of embryonic neural stem cells through YAP. J Neurosci, 34(36), 12039–12048. doi:10.1523/JNEUROSCI.0486-14.2014 [PubMed: 25186749]

Zawadzka M, Rivers LE, Fancy SP, Zhao C, Tripathi R, Jamen F, . . . Franklin RJ (2010). CNS-resident glial progenitor/stem cells produce Schwann cells as well as oligodendrocytes during repair of CNS demyelination. Cell Stem Cell, 6(6), 578–590. doi:10.1016/j.stem.2010.04.002 [PubMed: 20569695]

Zhang Y, Chen K, Sloan SA, Bennett ML, Scholze AR, O'Keeffe S, . . . Wu JQ (2014). An RNA-sequencing transcriptome and splicing database of glia, neurons, and vascular cells of the cerebral cortex. J Neurosci, 34(36), 11929–11947. doi:10.1523/JNEUROSCI.1860-14.2014 [PubMed: 25186741]

Main Points:

- YAP and TAZ are not required for myelin maintenance in the CNS.
- Ablation of YAP and TAZ in OLs significantly delays the remyelination process, suggesting that they are required for proper remyelination in the CNS.

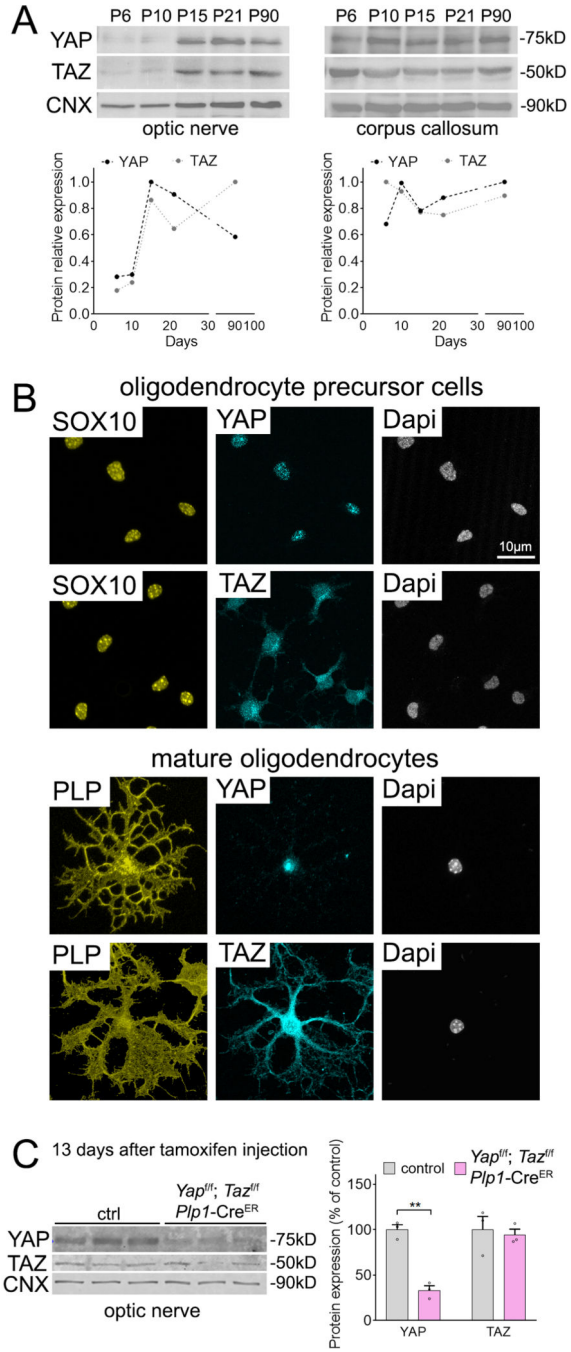

Figure 1.

YAP/TAZ are expressed by mouse OLs. (**A**) (top) Western blot analysis of YAP and TAZ in wildtype optic nerve (left) and corpus callosum (right) at 6, 10, 15, 21 and 30 days of age in mouse. Calnexin (CNX) was used as loading control. (bottom) Relative quantification of YAP and TAZ protein level from densitometries. (**B**) Immunolocalization of YAP and TAZ in OPC (SOX10+) (kept in proliferation conditions) and OL (PLP+) mouse cultures show localization of YAP and TAZ in OPC and OL nuclei and cytoplasm. Scale bar, 10 μm. (**C**) Western blot analysis of YAP and TAZ on optic nerve from *Yap*$^{f/f}$; *Taz*$^{f/f}$; *Plp1*-Cre^{ER}

animals, 13 days after treatment with tamoxifen, at 53 days of age. YAP protein levels are lower in *Yap*$^{f/f}$; *Taz*$^{f/f}$; *Plp1*-Cre^{ER} injected with tamoxifen compared to control *Yap*$^{f/f}$; *Taz*$^{f/f}$; *Plp1*-Cre^{ER}. CNX was used as loading control. n ≥ 3 mice for each condition. Protein expression data were normalized to the average of the control. Data are presented as mean ± s.e.m. Two-tailed Student's *t* test: **, *P*-value ≤ 0.01.

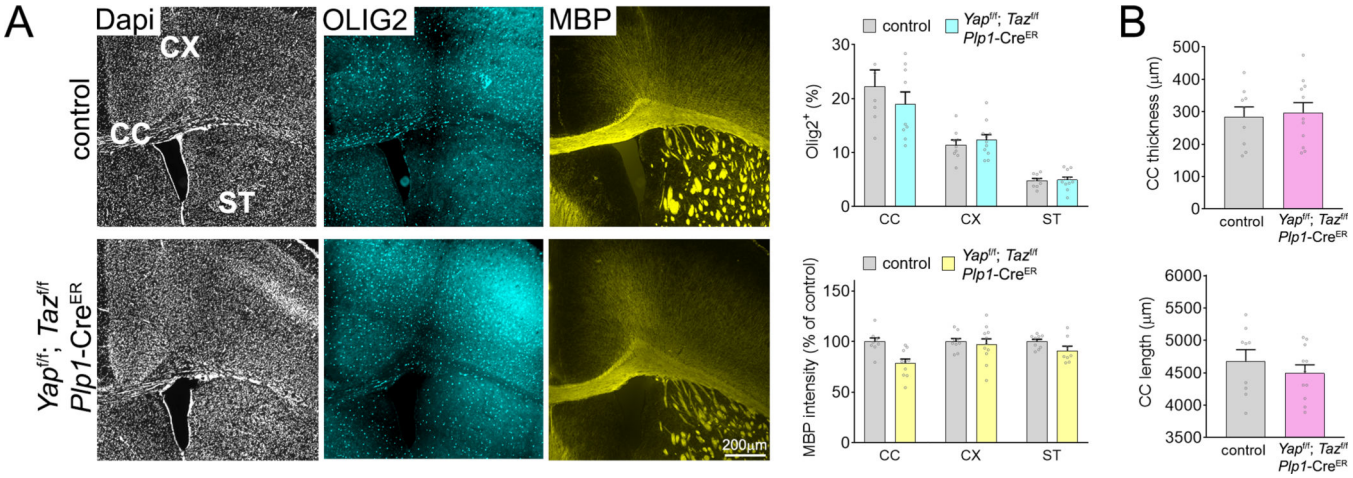

Figure 2.

MBP protein level and OLIG2-positive cell number are not affected in *Yap*$^{f/f}$; *Taz*$^{f/f}$; *Plp1*-Cre^{ER} brain. (**A**) (left) Representative coronal sections of brain tissue immunostained for MBP and OLIG2 collected from adult control and *Yap*$^{f/f}$; *Taz*$^{f/f}$; *Plp1*-Cre^{ER} animals, 13 days after treatment with tamoxifen, at 53 days of age. Scale bar, 200 μm. (right) Integrated fluorescence intensity for MBP and the number of OLIG2-positive cells were quantified in the lateral corpus callosum (CC), the cingulate cortex (CX) and striatum (ST). n ≥ 6 mice for each condition. (**B**) Corpus callosum length and midline thickness from adult control and *Yap*$^{f/f}$; *Taz*$^{f/f}$; *Plp1*-Cre^{ER} animals, 13 days after treatment with tamoxifen, at 53 days of age. n ≥ 8 mice for each condition. Intensity data were normalized to the average of the control for each brain region. Data are presented as mean ± s.e.m.

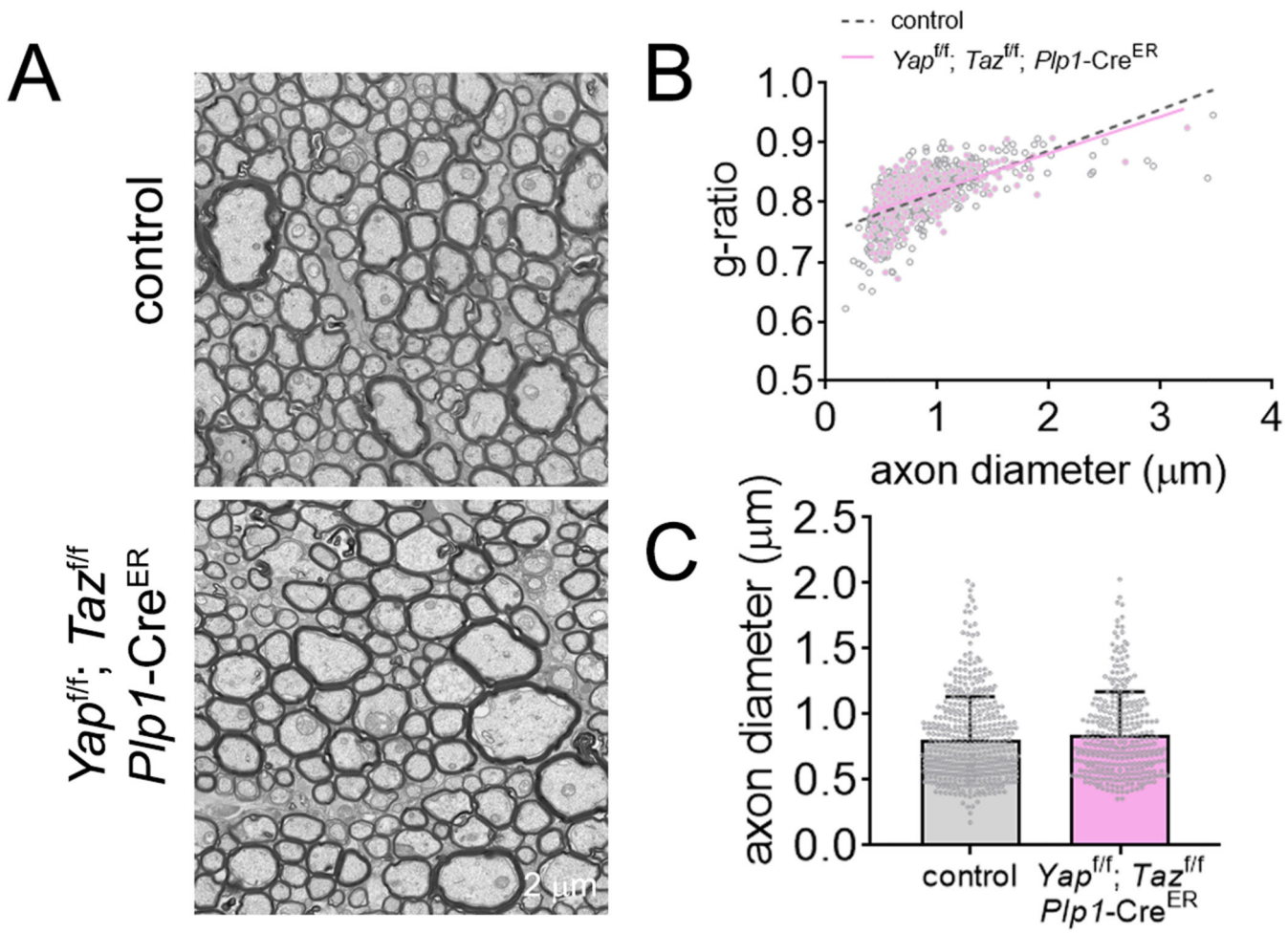

Figure 3.

Electron microscopy of the *Yap*$^{f/f}$; *Taz*$^{f/f}$; *Plp1*-Cre^{ER} optic nerve. (**A**) Electron micrographs of axons in the optic nerve of control and *Yap*$^{f/f}$; *Taz*$^{f/f}$; *Plp1*-Cre^{ER} mice, 13 days after treatment with tamoxifen, at 93 days of age. Scale bars, 2 µm. (**B**) Scatter plot of g-ratio values of myelinated axons. (**C**) Mean axonal diameter of myelinated axons. n > 100 fibers per animal were analyzed. Data are presented as mean ± s.d.

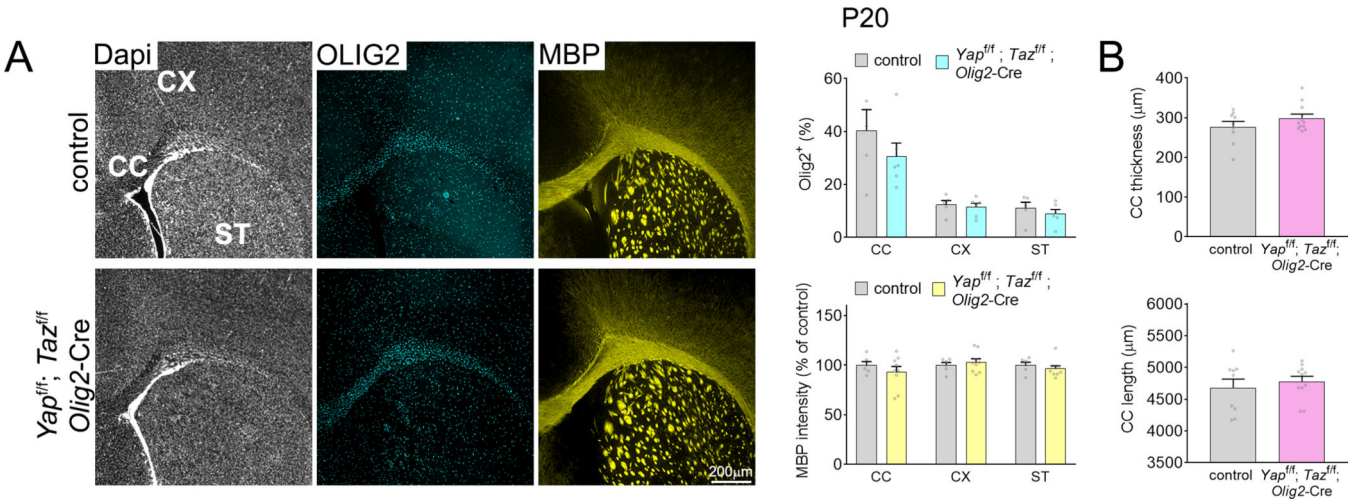

Figure 4.

MBP protein level and OLIG2-positive cell number are not affected in *Yap*$^{f/f}$; *Taz*$^{f/f}$; *Olig2*-Cre brain. (**A**) (left) Representative coronal sections of brain tissue immunostained for MBP and OLIG2 collected from adult control and *Yap*$^{f/f}$; *Taz*$^{f/f}$; *Olig2*-Cre animals, at 20 days of age. Scale bar, 200 µm. (right) Integrated fluorescence intensity for MBP and the number of OLIG2-positive cells were quantified in the lateral corpus callosum (CC), the cingulate cortex (CX) and striatum (ST). n ≥ 4 mice for each condition. (**B**) Corpus callosum length and midline thickness from adult control and *Yap*$^{f/f}$; *Taz*$^{f/f}$; *Olig2*-Cre animals, at 20 days of age. n ≥ 4 mice for each condition. Intensity data were normalized to the average of the control for each brain region. Data are presented as mean ± s.e.m.

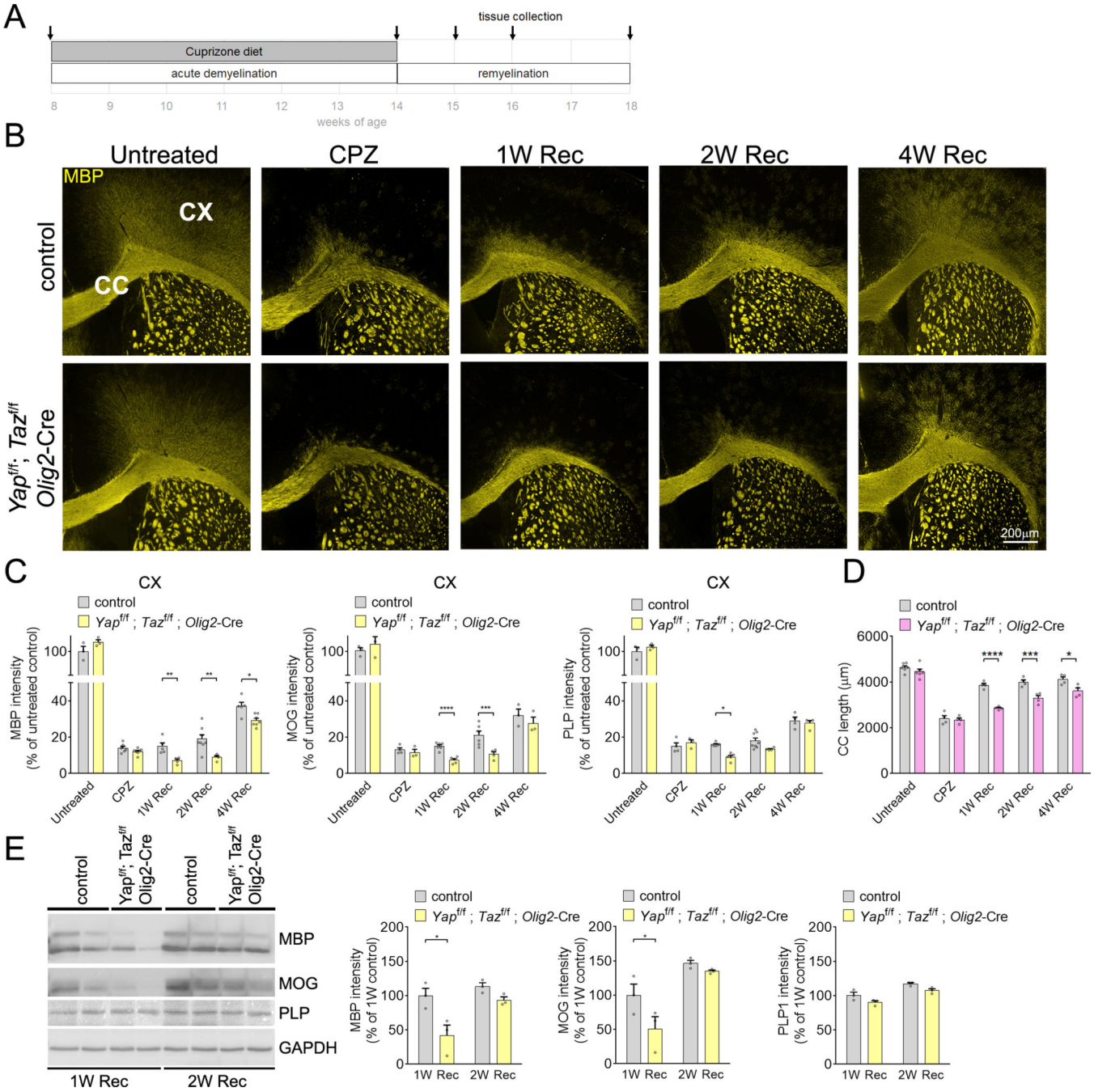

Figure 5.

Remyelination is delayed in the adult *Yap*$^{f/f}$; *Taz*$^{f/f}$; *Olig2*-Cre brain. (**A**) Schematic representative of the cuprizone treatment as well as sampling timepoints. (**B**) Representative coronal sections from control and *Yap*$^{f/f}$; *Taz*$^{f/f}$; *Olig2*-Cre brains immunostained for MBP. Tissues were collected from untreated, control, and *Yap*$^{f/f}$; *Taz*$^{f/f}$; *Olig2*-Cre mice at the end of the cuprizone (CPZ) treatment and after 1 week (1W Rec), 2 weeks (2W Rec) or 4 weeks of recovery (4W Rec). Scale bar, 200 μm. (**C**) Integrated fluorescence intensity for MBP, MOG and PLP were quantified in the cortex (CX) of untreated, control, and *Yap*$^{f/f}$; *Taz*$^{f/f}$;

Olig2-Cre mice at the end of the CPZ treatment and after 1, 2 and 4 weeks of recovery. Fluorescent intensity data are presented as percent of untreated control mice. (**D**) Western blot analysis of MBP and MOG on cortex from control and *Yap*$^{f/f}$; *Taz*$^{f/f}$; *Olig2*-Cre animals, 1 or 2 weeks after CPZ withdrawal. MBP and MOG protein levels are lower in *Yap*$^{f/f}$; *Taz*$^{f/f}$; *Olig2*-Cre, after 1 week of recovery. GAPDH was used as loading control. n ≥ 3 mice for each condition. IHC intensity data were normalized to the average of the untreated control. WB intensity data were normalized to the average of the control for each brain region. Data are presented as mean ± s.e.m. Two-tailed Student's *t* test: *, *P*-value ≤ 0.05; **, *P*-value ≤ 0.01; ****, *P*-value ≤ 0.0001.

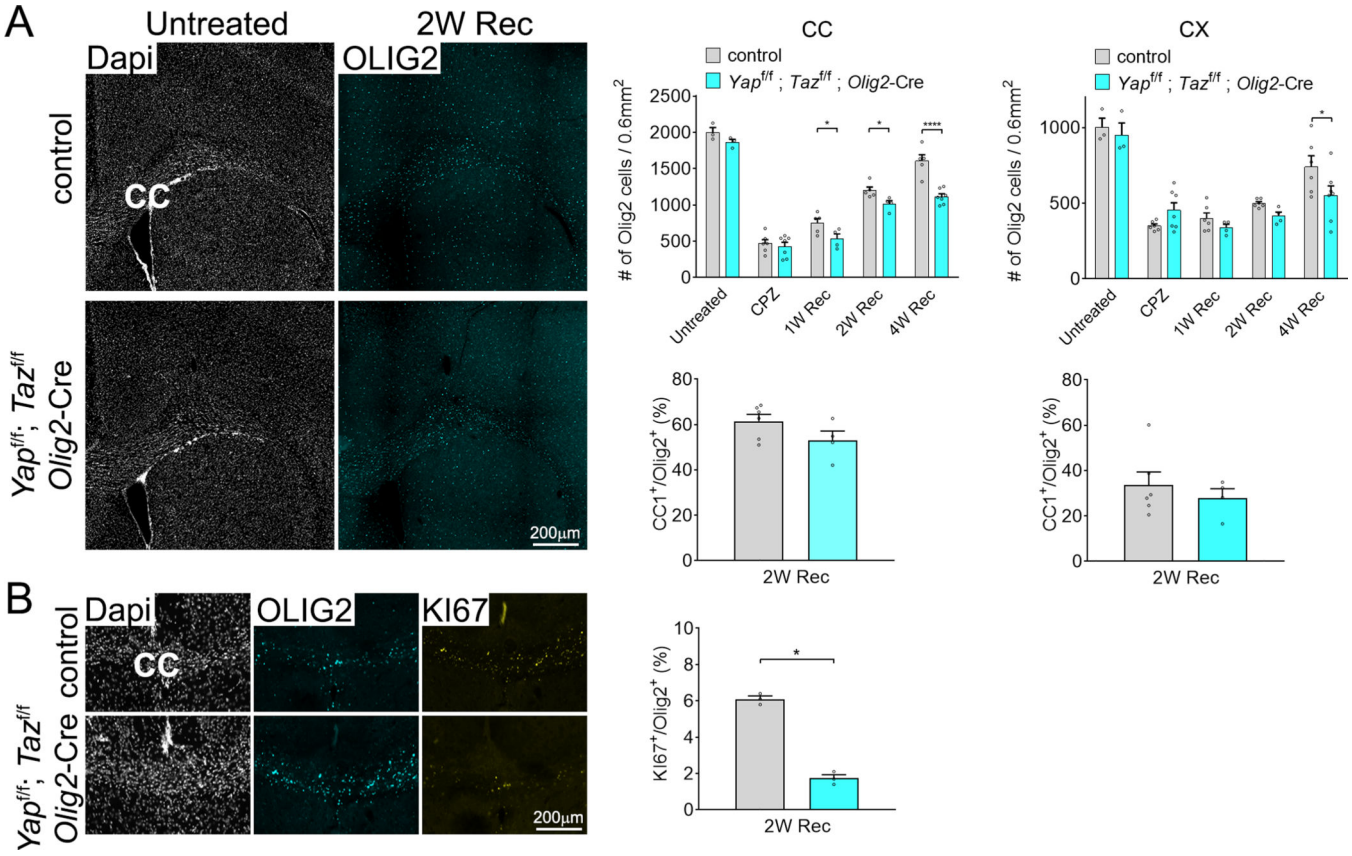

Figure 6.

Oligodendrocyte proliferation is reduced in the corpus callosum of *Yap*$^{f/f}$; *Taz*$^{f/f}$; *Olig2*-Cre animal during remyelination. (**A**) The number of OLIG2-positive, and CC1-positive cells were quantified in the corpus callosum and cortex of control, and *Yap*$^{f/f}$; *Taz*$^{f/f}$; *Olig2*-Cre mice at the end of the CPZ treatment and after 1, 2 and 4 weeks of recovery. (**B**) The number of KI67-positive cells were quantified in the corpus callosum of control, and *Yap*$^{f/f}$; *Taz*$^{f/f}$; *Olig2*-Cre mice after 2 weeks of recovery. n ≥ 3 mice for each condition. CC1+/Olig2+ and KI67+/Olig2+ data are represented as percentage of Olig2+ cells. Data are presented as mean ± s.e.m. Two-tailed Student's *t* test: *, *P*-value ≤ 0.05; ****, *P*-value ≤ 0.0001.